PAPER

Iterative Reduction of Out-of-Band Power and Peak-to-Average Power Ratio for Non-Contiguous OFDM Systems Based on POCS*

Yanqing LIU[†a)], ***Member and*** **Liang DONG**[††], ***Nonmember***

SUMMARY Non-contiguous orthogonal frequency-division multiplexing (OFDM) is a promising technique for cognitive radio systems. The secondary users transmit on the selected subcarriers to avoid the frequencies being used by the primary users. However, the out-of-band power (OBP) of the OFDM-modulated tones induces interference to the primary users. Another major drawback of OFDM-based system is their high peak-to-average power ratio (PAPR). In this paper, algorithms are proposed to jointly reduce the OBP and the PAPR for non-contiguous OFDM based on the method of alternating projections onto convex sets. Several OFDM subcarriers are selected to accommodate the adjusting weights for OBP and PAPR reduction. The frequency-domain OFDM symbol is projected onto two convex sets that are defined according to the OBP requirements and the PAPR limits. Each projection iteration solves a convex optimization problem. The projection onto the set constrained by the OBP requirement can be calculated using an iterative algorithm which has low computational complexity. Simulation results show good performance of joint reduction of the OBP and the PAPR. The proposed algorithms converge quickly in a few iterations.

key words: *non-contiguous OFDM, out-of-band power suppression, PAPR reduction, alternating projections onto convex sets*

1. Introduction

Non-contiguous orthogonal frequency-division multiplexing (NC-OFDM) is a multicarrier modulation technique that can be used for cognitive radio systems [1]–[3]. The secondary users transmit on the selected OFDM subcarriers to avoid the frequencies being used by the primary users. The OFDM-based cognitive radio network has high spectrum efficiency with closely spaced orthogonal subcarrier signals. It combats the dispersion effect of the multipath channel and simplifies the receiver equalizer. However, the out-of-band radiation in OFDM transmission interferes with wireless communications in adjacent channels and endangers the co-existence with the incumbent radio systems. There are several methods to reduce the out-of-band power (OBP). Cosovic and Mazzoni put forward a method of multiple choice sequences [4]. It transforms the original transmit sequence into a set of sequences and chooses the one with the lowest OBP. Cancellation subcarriers can be used at the edges of the NC-OFDM bands. Yuan and Wyglinski proposed a method of combining cancellation subcarriers and modulated filter banks to suppress the sidelobes [5]. Pagadarai et al. used a method of constellation expansion to reduce the OBP [6]. It is computationally efficient and no side information is needed. Li et al. proposed a method to reduce the OBP by iteratively adjusting the constellation points for the subcarriers that are close to the edges of the used bandwidth [7]. Zhang et al. used an orthogonal projection method to suppress the sidelobes of the multicarrier systems [8]. Mahmoud et al. put forward a method to extend OFDM symbols to minimize the adjacent channel interference [9]. van de Beek proposed a multiplexing scheme to shape the signal's transmit spectrum [10]. Another major drawback of the OFDM-based systems is their high peak-to-average power ratio (PAPR). Krongold and Jones proposed an active-set method, which reserved tones to design a peak-cancelling signal that lowers the PAPR of a transmit OFDM block [11].

These methods mentioned above deal with the OBP and the PAPR problems separately. But optimizing the OBP or the PAPR affect each other. Reducing one may increase the other. In this paper, we reduce the OBP and the PAPR jointly. Some methods have already been proposed to address the problem. Li et al. investigated the effects of clipping and filtering on the performance of OFDM [12]. Senst et al. proposed a joint optimization method that reserves a subset of the OFDM subcarriers for the task [13]. A parameter is used to control the trade-off between the reduction of the OBP and that of the PAPR. Ghassemi et al. proposed a method of joint reduction of the OBP and the PAPR using selected mapping [14]. Multiple representations of the transmit signal are generated and a sequence with relatively low OBP and PAPR is selected. Their method requires transmitting additional phasor information in order for the receiver to select the correct OFDM symbol. Ni et al. proposed a signal cancellation method for joint PAPR reduction and OBP suppression in NC-OFDM-based cognitive radio systems [15]. Some of the constellation points are dynamically extended on the secondary user subcarriers and several signal-cancellation symbols are added on the primary user subcarriers. The problem is formulated as a quadratically constrained quadratic program and the cancellation signal is obtained by convex optimization.

In this paper, we propose algorithms of joint reduction of the OBP and the PAPR for NC-OFDM that are based on alternating projections onto convex sets (POCS). Several

Manuscript received August 19, 2016.
Manuscript revised January 4, 2017.
Manuscript publicized February 17, 2017.

[†]The author is with the Department of Communication Engineering, Jiangxi University of Finance and Economics, China.
[††]The author is with the Department of Electrical and Computer Engineering, Baylor University, USA.

*This work was supported in part by the National Natural Science Foundation of China under Grant 61661022.

a) E-mail: yanqing_liu_baylor@126.com

DOI: 10.1587/transcom.2016EBP3326

OFDM subcarriers including all the primary user subcarriers, are selected to accommodate the adjusting weights to reduce the OBP and the PAPR. The adjusting weight vector is refined by iteratively projecting the frequency-domain OFDM symbol onto two convex sets. These two convex sets are respectively defined by the OBP and the PAPR constraints. The projection onto the set regulated by the OBP requirement is decomposed so that an iterative method can be applied and no convex optimization tools are needed. The projection onto the set regulated by the PAPR condition has no analytical solution and convex optimization tools are used. Algorithm convergence is guaranteed by the property of the POCS. Based on the priorities of the OBP requirement and the PAPR requirement, two algorithms are proposed. Algorithm 1 converges to a signal vector that satisfies the OBP requirement and is the closest to the set regulated by the PAPR requirement. Algorithm 2 converges to a signal vector that satisfies the PAPR requirement and is the closest to the set regulated by the OBP requirement.

The clipping and filtering method reduces the sidelobe power outside of the whole OFDM subcarriers. And, the clipping process causes the in-band signal distortion, which degrades the bit error rate (BER) performance. Compared to the clipping and filtering method, the methods proposed suppress the sidelobe power of the NC-OFDM-based cognitive radio system in the band where the primary user subcarriers locate to create a spectrum notches, and does not introduce in-band signal distortion. Compared with the method in [13], our algorithms do not need a trade-off parameter to control the relative priority of the OBP and the PAPR requirements. The method in [13] needs to solve a complex convex optimization problem. In this paper, an algorithm is proposed to solve the projection onto the set constrained by the OBP limit, which reduces the complexity. Compared with the method in [15], we reserve some tones to control the OBP and the PAPR. The method in [15] does not need to reserve tones. However, by extending the constellation points in specific directions, it increases the total transmit power. With preliminary results reported in our conference paper [16], this paper has substantially extended work in the following aspects. First, the primary user subcarriers are selected to carry optimizing weights to improve the performance. In our conference paper, the weights on the primary subcarriers are set to zero. Second, the performances of the algorithms are compared against each other and against other methods such as the constellation extension method. Third, the projection onto the set controlled by the OBP limit is decomposed, and an iterative method to solve the projection is proposed. This method is less complex compared to the method in our conference paper. Fourth, we study a practical NC-OFDM system with the cyclic prefix and the interpolation filter. The PAPR is calculated through oversampling.

2. System Model and Problem Formulation

2.1 Models of OBP and PAPR

In a cognitive radio system that employs the NC-OFDM modulation technique, the secondary users of the spectrum transmit data on the selected subcarriers. With spectrum sensing, these subcarriers are not located in the frequency band that is occupied by the incumbent primary users. The selected subcarriers are active for secondary data transmission while other OFDM subcarriers are not used to send data to avoid interference to the primary users. The discrete-time baseband OFDM signal in the time domain is given by

$$x[n] = x_n = \frac{1}{\sqrt{N}} \sum_{k=0}^{N-1} X_k e^{j2\pi \frac{kn}{N}}, \quad n = 0, \cdots, N-1 \quad (1)$$

where N is the number of the OFDM subcarriers. The subcarrier spacing is $1/(NT_s)$, where T_s is the sampling period and NT_s is the OFDM symbol period. $\{X_k\}_{k=0}^{N-1}$ are the data on the subcarriers.

In order to calculate the OBP in real transmissions, we need to examine the analog baseband signal. Cyclic prefix (CP) is used to combat the inter-symbol interference (ISI) caused by multipath. The analog signal $x(t)$ is obtained by feeding the discrete-time signal x_n to an interpolation filter $g_I(t)$ as

$$x(t) = g_I(t) * \left(\sum_{n=-N_{cp}}^{N-1} x_n \delta(t - nT_s) \right) \quad (2)$$

where N_{cp} is the length of the CP. The energy spectrum of $x(t)$ is given by

$$\psi(f) = \frac{L^2}{N} \left| G_I(f) \sum_{k=0}^{N-1} X_k \mathrm{sinc}_{\mathrm{L}}(f - f_k) \right. \\ \left. e^{-j\pi(f-f_k)T_s(L-2N_{cp}-1)} \right|^2 \quad (3)$$

where $L = N + N_{cp}$ and $f_k = k/NT_s$. $G_I(f)$ is the Fourier transform of interpolation filter $g_I(t)$, and the function $\mathrm{sinc}_{\mathrm{L}}$ is defined as

$$\mathrm{sinc}_{\mathrm{L}}(f) = \begin{cases} \frac{\sin(\pi L T_s f)}{L \sin(\pi T_s f)}, & T_s f \notin \mathbb{Z} \\ (-1)^{T_s f (L-1)}, & \text{otherwise} \end{cases} \quad (4)$$

where $\mathbb{Z}$ is the set of integers. In some literature, a sinc function is used in the expression of the energy spectrum. However, as revealed in (2), a sampled rectangular window is applied to the time-domain signal. The spectrum of a sampled rectangular window is not a sinc function but a periodic function sinc_L [17]–[19]. The phase information needs to be considered as in (3).

The energy in the out-of-band of the NC-OFDM subcarriers is given by

$$E_{\mathrm{OB}} = \int_{f \in \mathcal{G}} \psi(f) df \quad (5)$$

where $\mathcal{G}$ denotes the intervals of out-of-band frequency. We approximate E_{OB} by using M evenly spaced frequency samples $\{g_m\}_{m=1}^{M}$ in $\mathcal{G}$, therefore

$$E_{\mathrm{OB}} \approx \frac{L^2}{N} \triangle_g \sum_{m=1}^{M} \left| G_I(g_m) \sum_{k=0}^{N-1} X_k \mathrm{sinc_L}(g_m - f_k) e^{-j\pi(g_m - f_k)T_s(L-2N_{cp}-1)} \right|^2 \quad (6)$$

where $\triangle_g$ is the spacing between any two adjacent frequency samples. The OBP is linearly proportional to E_{OB}. To formulate the optimization problem, we normalize the OBP by setting the linear constant to 1. It follows that

$$\mathrm{OBP} = \sum_{m=1}^{M} \left| G_I(g_m) \sum_{k=0}^{N-1} X_k \mathrm{sinc_L}(g_m - f_k) e^{-j\pi(g_m - f_k)T_s(L-2N_{cp}-1)} \right|^2 \quad (7)$$

$$= \|\mathbf{SX}\|_2^2 \quad (8)$$

where $\mathbf{S}$ is a $M \times N$ matrix that is given by

$$\mathbf{S} = \begin{pmatrix} S(g_1 - f_0) & S(g_1 - f_1) & \cdots & S(g_1 - f_{N-1}) \\ S(g_2 - f_0) & S(g_2 - f_1) & \cdots & S(g_2 - f_{N-1}) \\ \vdots & \vdots & \ddots & \vdots \\ S(g_M - f_0) & S(g_M - f_1) & \cdots & S(g_M - f_{N-1}) \end{pmatrix}$$

where $S(g-f) = G_I(g)\mathrm{sinc_L}(g-f)e^{-j\pi(g-f)T_s(L-2N_{cp}-1)}$, f_k is the normalized subcarrier frequency, and g_m is the normalized frequency sample within the OBP measurement range. $\mathbf{X} = [X_0, X_1, \ldots, X_{N-1}]^T$.

We use J-times oversampling to calculate the PAPR of an NC-OFDM symbol. The oversampled discrete-time baseband OFDM signal is given by

$$x[n] = x_n = \frac{1}{\sqrt{N}} \sum_{k=0}^{N-1} X_k e^{j2\pi \frac{kn}{JN}}, \quad n = 0, \cdots, JN-1. \quad (9)$$

The discrete-time baseband signal can be written as

$$\mathbf{x} = \mathbf{FX} \quad (10)$$

where $\mathbf{F}$ is the $JN \times N$ inverse discrete Fourier transform (IDFT) matrix. The PAPR of an OFDM symbol can be estimated by

$$\mathrm{PAPR} = \frac{\max |x_n|^2}{\mathrm{E}[|x_n|^2]} \quad (11)$$

where $\mathrm{E}[\cdot]$ denotes the expectation. Usually, the oversampling factor J can take an integer with $J \geq 4$ for the PAPR estimate in (11) to approach the actual PAPR of the continuous-time signal. We assume that the energy of an OFDM symbol is approximately constant. Therefore, limiting the PAPR is equivalent to limiting $\|\mathbf{x}\|_\infty$.

2.2 Problem Formulation of OBP and PAPR Reduction

Adjacent selected NC-OFDM subcarriers are grouped into data blocks. Similar to the approaches in [5], [13], in each data block, several subcarriers are dedicated to the joint reduction of the OBP and the PAPR. Similar to [15], all the primary user subcarriers accommodate adjusting weights. Let $\mathcal{W}$ denote the index set of these adjusting subcarriers. The adjusting weights are $\{w_k\}$, $k \in \mathcal{W}$. The number of adjusting subcarriers influences the effective data rate. The rate loss increases with more adjusting subcarriers. Let $\mathcal{D}$ denote the index set of the NC-OFDM subcarriers that carry data. The transmitted signals on the data subcarriers are $\{d_k\}$, $k \in \mathcal{D}$. Define complex weight vector $\mathbf{w} \in \mathbb{C}^{N\times 1}$ with nonzero elements at $\mathcal{W}$, such that

$$\mathbf{w}[k] = \begin{cases} w_k, & k \in \mathcal{W} \\ 0, & k \notin \mathcal{W}. \end{cases} \quad (12)$$

Define complex data vector $\mathbf{d} \in \mathbb{C}^{N\times 1}$ with nonzero elements at $\mathcal{D}$, such that

$$\mathbf{d}[k] = \begin{cases} d_k, & k \in \mathcal{D} \\ 0, & k \notin \mathcal{D}. \end{cases} \quad (13)$$

Consequently, the NC-OFDM signal in the frequency domain is given by

$$\mathbf{X} = \mathbf{d} + \mathbf{w}. \quad (14)$$

The adjusting subcarriers are allocated according to the following rules. For each NC-OFDM data block, the subcarriers on the edges are assigned weights in order to reduce the OBP. Some subcarriers in the middle of the NC-OFDM data block and all the subcarriers of the primary users are assigned weights to reduce the PAPR. Before system implementation, detailed allocations of the adjusting subcarriers can be tested and the number and the indexes of the adjusting subcarriers are determined offline taking into account the trade-off between the OBP and the PAPR and the efficiency of data transmission.

The block diagrams of the transmitter and the receiver are shown in Fig. 1 and Fig. 2, respectively. At the transmitter, based on the data vector $\mathbf{d}$, special algorithms are required to determine the weight vector $\mathbf{w}$. At the receiver, no system modification is needed and the data are extracted from the NC-OFDM symbol. The problem of tuning the weight vector $\mathbf{w}$ to regulate the OBP and the PAPR can be formulated as

$$(\mathcal{P}_1): \begin{array}{ll} \text{find} & \mathbf{w} \in \mathbb{C}^{N\times 1} \\ \text{subject to} & \|\mathbf{Sw} + \mathbf{Sd}\|_2^2 \leq P_{\mathrm{OBP}} \\ & \|\mathbf{Fw} + \mathbf{Fd}\|_\infty \leq \Gamma_{\mathrm{PAPR}} \\ & (\mathbf{I} - \mathbf{I_w})\mathbf{w} = \mathbf{0} \end{array} \quad (15)$$

where P_{OBP} and Γ_{PAPR} are the limits according to the requirements of the OBP and the PAPR. $\mathbf{I}$ is the $N \times N$ identity matrix and $\mathbf{I_w}$ is an $N \times N$ diagonal matrix that is defined as

$$\mathbf{I_w}[i,i] = \begin{cases} 1, & i \in \mathcal{W} \\ 0, & i \notin \mathcal{W}. \end{cases} \quad (16)$$

$\mathbf{I_w}$ can be used to extract the nonzero elements of $\mathbf{w}$ whose

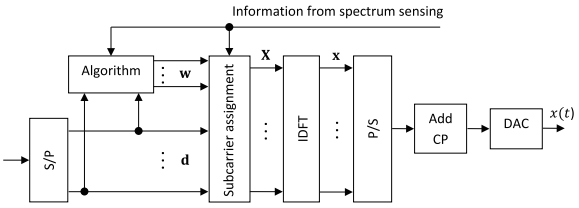

Fig. 1 Block diagram of the NC-OFDM transmitter.

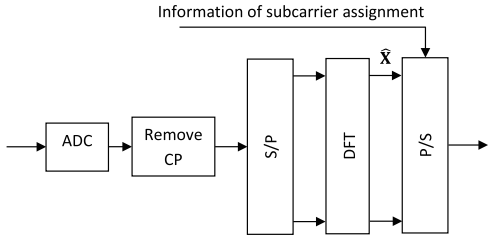

Fig. 2 Block diagram of the NC-OFDM receiver.

indexes are in $\mathcal{W}$. Problem $\mathcal{P}_1$ can be further written as

$$(\mathcal{P}_1): \quad \begin{array}{ll} \text{find} & \mathbf{X} \in \mathbb{C}^{N\times 1} \\ \text{subject to} & \|\mathbf{SX}\|_2^2 \le P_{\text{OBP}} \\ & \|\mathbf{FX}\|_\infty \le \Gamma_{\text{PAPR}} \\ & (\mathbf{I}-\mathbf{I_w})\mathbf{X} = \mathbf{d}. \end{array} \tag{17}$$

Problem $\mathcal{P}_1$ may not be feasible, because the OBP and the PAPR requirements may not be simultaneously satisfied. In the next section, we solve the problem with the method of alternating projections onto convex sets (POCS).

3. Iterative Reduction of OBP and PAPR Using POCS

3.1 Alternating Projections onto Convex Sets

Thanks to its effectiveness, POCS has been applied in many fields such as image restoration and signal synthesis. Let $\mathcal{S}$ be a convex set, the projection operator of vector $\mathbf{g}$ onto $\mathcal{S}$ is defined as

$$\pi_{\mathcal{S}}(\mathbf{g}) = \underset{\mathbf{f}\in\mathcal{S}}{\text{argmin}} \|\mathbf{g}-\mathbf{f}\|_2. \tag{18}$$

If two closed convex sets have intersection, alternately projecting a vector onto these sets will converge to a common vector point in these sets [20]. If two closed convex sets have no intersection, alternately projecting a vector onto these sets will converge to a line segment in between these sets. Each of the two end points is in one set and closest to the other set [21], [22]. If there are three or more closed convex sets that have no intersection, the alternating projection method will converge to a limit cycle in between these sets [22], [23]. The method of simultaneous weighted projections can be used to find a compromise solution with the constraints defined by the non-intersecting convex sets.

3.2 Algorithms of Iterative Reduction of OBP and PAPR Based on POCS

When POCS is used to solve Problem $\mathcal{P}_1$, the frequency-domain signal $\mathbf{X}$ can be regarded as the vector that is to be projected onto the convex sets. Define Set $\mathcal{A}$ as

$$\mathcal{A} = \{\mathbf{X} \mid \|\mathbf{SX}\|_2^2 \le P_{\text{OBP}}, (\mathbf{I}-\mathbf{I_w})\mathbf{X} = \mathbf{d}\} \tag{19}$$

and define Set $\mathcal{B}$ as

$$\mathcal{B} = \{\mathbf{X} \mid \|\mathbf{FX}\|_\infty \le \Gamma_{\text{PAPR}}, (\mathbf{I}-\mathbf{I_w})\mathbf{X} = \mathbf{d}\}. \tag{20}$$

Set $\mathcal{A}$ and Set $\mathcal{B}$ are convex sets, because the intersection of convex sets is convex [24]. Set $\mathcal{A}$ regulates the adjusting weights so that the OBP of the transmission is within the limit. Set $\mathcal{B}$ regulates the adjusting weights so that the PAPR is within the limit. We assume that neither $\mathcal{A}$ nor $\mathcal{B}$ is empty.

Define the operator of projection onto convex Set $\mathcal{A}$ as

$$\pi_{\mathcal{A}}(\mathbf{X}) = \underset{\mathbf{X}'\in\mathcal{A}}{\text{argmin}} \|\mathbf{X}-\mathbf{X}'\|_2. \tag{21}$$

The solution of operation $\pi_{\mathcal{A}}(\mathbf{X})$ can be obtained by solving the following convex optimization problem:

$$\begin{array}{ll} \underset{\mathbf{X}'}{\text{minimize}} & \|\mathbf{X}-\mathbf{X}'\|_2 \\ \text{subject to} & \|\mathbf{SX}'\|_2^2 \le P_{\text{OBP}} \\ & (\mathbf{I}-\mathbf{I_w})\mathbf{X}' = \mathbf{d}. \end{array} \tag{22}$$

In Sect. 3.3, we exploit the structure of problem (22) and propose an iterative algorithm to solve it, which avoids using complex convex optimization tools.

Define the operator of projection onto convex Set $\mathcal{B}$ as

$$\pi_{\mathcal{B}}(\mathbf{X}) = \underset{\mathbf{X}'\in\mathcal{B}}{\text{argmin}} \|\mathbf{X}-\mathbf{X}'\|_2. \tag{23}$$

The solution of operation $\pi_{\mathcal{B}}(\mathbf{X})$ can be obtained by solving the following convex optimization problem:

$$\begin{array}{ll} \underset{\mathbf{X}'}{\text{minimize}} & \|\mathbf{X}-\mathbf{X}'\|_2 \\ \text{subject to} & \|\mathbf{FX}'\|_\infty \le \Gamma_{\text{PAPR}} \\ & (\mathbf{I}-\mathbf{I_w})\mathbf{X}' = \mathbf{d}. \end{array} \tag{24}$$

Problem (24) cannot be decomposed into a simpler form, and convex optimization tools need to be used to solve it.

We propose algorithms of joint reduction of OBP and PAPR based on the method of POCS, which is described in Algorithm 1 and Algorithm 2. Since both $\mathcal{A}$ and $\mathcal{B}$ are convex sets, the projection onto either set is a convex optimization problem. According to the properties of the POCS, Algorithm 1 converges to a signal vector that has the desired weight $\mathbf{w}$ if $\mathcal{A}$ and $\mathcal{B}$ have intersection. If $\mathcal{A}$ and $\mathcal{B}$ have no intersection, the algorithm converges to a limit cycle that corresponds to the shortest distance between the two sets. In Algorithm 1 in particular, the alternating process stops after it converges and vector $\mathbf{X}$ is projected onto Set $\mathcal{A}$. Therefore, the algorithm converges to a signal vector that satisfies the constraint imposed by the OBP regulation and is closest to the set constrained by the PAPR limit. In Algorithm 2, regulating the PAPR has higher priority. The alternating projection process stops and vector $\mathbf{X}$ is finally projected onto the set controlled by the PAPR limit. The

Algorithm 1 Joint reduction of OBP and PAPR based on POCS with OBP reduction having higher priority

1. Initialize $\mathbf{w} = \mathbf{w}_0$ and $\mathbf{X} = \mathbf{d} + \mathbf{w}_0$;
2. Project $\mathbf{X}$ onto $\mathcal{B}$, that is $\mathbf{X} = \pi_{\mathcal{B}}(\mathbf{X})$;
3. Project $\mathbf{X}$ onto $\mathcal{A}$, that is $\mathbf{X} = \pi_{\mathcal{A}}(\mathbf{X})$;
4. Go to Step 2 until it converges to a vector point or a limit cycle.

Algorithm 2 Joint reduction of OBP and PAPR based on POCS with PAPR reduction having higher priority

1. Initialize $\mathbf{w} = \mathbf{w}_0$ and $\mathbf{X} = \mathbf{d} + \mathbf{w}_0$;
2. Project $\mathbf{X}$ onto $\mathcal{A}$, that is $\mathbf{X} = \pi_{\mathcal{A}}(\mathbf{X})$;
3. Project $\mathbf{X}$ onto $\mathcal{B}$, that is $\mathbf{X} = \pi_{\mathcal{B}}(\mathbf{X})$;
4. Go to Step 2 until it converges to a vector point or a limit cycle.

solution vector meets the PAPR requirement and is closest to the set constrained by the OBP constraint. Moreover, the method of simultaneous weighted projections can be used to find a compromise solution with the constraints defined by the two convex sets.

For the above two algorithms, the target PAPR and OBP limits should not be too small. If PAPR or OBP constraints are set too tight, the set constrained will be empty for specific data need to be transmitted; thus, there will be no valid set to be projected onto. We assume that before system implementation, the target OBP and PARP limits can be determined by simulation in order to guarantee set A and B are not empty. Normally, we cannot guarantee that the sets controlled by the target OBP and target PAPR have intersection. It means the algorithms cannot converge to target OBP and PAPR values simultaneously. In reality, giving priority to the OBP performance or the PAPR performance need to be determined. Then Algorithm 1 or Algorithm 2 can be applied. The target OBP and PAPR limits can then be predetermined by simulation considering keeping balance between the performance of the OBP and PAPR. For Algorithm 1, the alternating process stops after the projection onto the set constrained by the target OBP limit; therefore, the OBP performance depends on the OBP target limit. Normally, the target OBP and target PAPR performance cannot be achieved simultaneously. Reducing one causes increasing the other. Thus, looser OBP target limit causes better PAPR performance. Similarly, for Algorithm 2, the PAPR performance depends on the PAPR target limit, and looser target PAPR limit causes better OBP performance. The number of adjusting subcarriers also influences the achievable PAPR and OBP. Let $|\mathcal{D}|$ and $|\mathcal{W}|$ denote the cardinalities of Set $\mathcal{D}$ and Set $\mathcal{W}$, respectively. When the ratio of $|\mathcal{D}|$ and $|\mathcal{W}|$ is smaller, which means there are more adjusting subcarriers, tighter target PAPR and OBP limits can be set, because there are more weights that can be adjusted to satisfy the PAPR and OBP constraints. Therefore, a better PAPR and OBP performance can be achieved. However, smaller ratio of $|\mathcal{D}|$ and $|\mathcal{W}|$ means less data subcarriers, and lower data rate. Determining the number of adjusting subcarriers should balance between the PAPR and OBP performance and the efficiency of data transmission.

Algorithm 3 Projection onto Set $\mathcal{A}$

1. Initialize λ_{max} and λ_{min};
2. Calculate $(\lambda_{min} + \lambda_{max})/2$;
3. Calculate $\check{\mathbf{w}}^*$, according to (31);
4. If $P_{\text{OBP}} < \|\mathbf{S}\mathbf{T}_{\mathbf{w}}\check{\mathbf{w}}^* + \mathbf{S}\mathbf{d}\|_2^2$, let $\lambda_{min} = \lambda$; otherwise let $\lambda_{max} = \lambda$;
5. Repeat from Step 2 until λ converges, that is, $\lambda_{max} - \lambda_{min}$ is smaller than a threshold;
6. $\mathbf{w} = \mathbf{T}_{\mathbf{w}}\check{\mathbf{w}}^*$ and $\mathbf{X} = \mathbf{d} + \mathbf{w}$.

3.3 Projection onto Set $\mathcal{A}$ with OBP Constraint

We develop a method to solve the convex optimization problem of the projection onto Set $\mathcal{A}$ constrained by the OBP condition. Let $\check{\mathbf{w}}$ and $\check{\mathbf{w}}'$ be two $N_w \times 1$ vectors. $N_w = |\mathcal{W}|$, where $|\mathcal{W}|$ is the cardinality of Set $\mathcal{W}$. $\check{\mathbf{w}}$ and $\check{\mathbf{w}}'$ are the vectors that squeeze out zeros from $\mathbf{w}$ and $\mathbf{w}'$, respectively, and leave only the adjusting weights on positions $\mathcal{W}$. For example, $\mathbf{w} = [w_1, 0, 0, w_2]^T$, $\check{\mathbf{w}} = [w_1, w_2]^T$. Projection onto Set $\mathcal{A}$ (21) is equivalent to the following optimization problem.

$$\begin{aligned} \underset{\check{\mathbf{w}}'}{\text{minimize}} \quad & \|\check{\mathbf{w}} - \check{\mathbf{w}}'\|_2^2 \\ \text{subject to} \quad & \|\mathbf{S}\mathbf{T}_{\mathbf{w}}\check{\mathbf{w}}' + \mathbf{S}\mathbf{d}\|_2^2 \le P_{\text{OBP}} \end{aligned} \tag{25}$$

where $\mathbf{T}_{\mathbf{w}}$ is a $N \times N_w$ matrix that recovers $\mathbf{w}$ from $\check{\mathbf{w}}$ as

$$\mathbf{w} = \mathbf{T}_{\mathbf{w}}\check{\mathbf{w}}. \tag{26}$$

For example, if $\mathbf{w} = [w_1, 0, 0, w_2]$, then

$$\mathbf{T}_{\mathbf{w}} = \begin{pmatrix} 1 & 0 \\ 0 & 0 \\ 0 & 0 \\ 0 & 1 \end{pmatrix}.$$

The Karush–Kuhn–Tucker (KKT) conditions [24] of Problem (25) are given by

$$-2(\check{\mathbf{w}} - \check{\mathbf{w}}^*) + \lambda(2\mathbf{T}_{\mathbf{w}}^H\mathbf{S}^H(\mathbf{S}\mathbf{T}_{\mathbf{w}}\check{\mathbf{w}}^* + \mathbf{S}\mathbf{d})) = \mathbf{0} \tag{27}$$

$$\|\mathbf{S}\mathbf{T}_{\mathbf{w}}\check{\mathbf{w}}^* + \mathbf{S}\mathbf{d}\|_2^2 \le P_{\text{OBP}} \tag{28}$$

$$\lambda \ge 0 \tag{29}$$

$$\lambda(\|\mathbf{S}\mathbf{T}_{\mathbf{w}}\check{\mathbf{w}}^* + \mathbf{S}\mathbf{d}\|_2^2 - P_{\text{OBP}}) = 0 \tag{30}$$

where $\check{\mathbf{w}}^*$ is the optimal solution and λ is the dual variable with respect to the OBP constraint. Given λ, it follows (27) that

$$\check{\mathbf{w}}^* = (\mathbf{I} + \lambda\mathbf{T}_{\mathbf{w}}^H\mathbf{S}^H\mathbf{S}\mathbf{T}_{\mathbf{w}})^{-1}(\check{\mathbf{w}} - \lambda\mathbf{T}_{\mathbf{w}}^H\mathbf{S}^H\mathbf{S}\mathbf{d}). \tag{31}$$

And λ can be updated with a bisection method. The algorithm to calculate the projected vector onto Set $\mathcal{A}$ that has the desired $\mathbf{w}$ can be described as Algorithm 3.

3.4 Complexity Analysis

The computational complexity of the projection onto Set $\mathcal{A}$ is indicated by the number of real multiplications it requires. Algorithm 1 and Algorithm 2 use the method in

Sect. 3.3 to project the signal vector onto Set $\mathcal{A}$. The optimal weight vector $\check{\mathbf{w}}$ is calculated according to (31). In practice, the values of $\mathbf{T}_\mathbf{w}^H\mathbf{S}^H\mathbf{S}\mathbf{T}_\mathbf{w}$ and $\mathbf{T}_\mathbf{w}^H\mathbf{S}^H\mathbf{S}$ can be pre-calculated and stored, because matrices $\mathbf{T}_\mathbf{w}$ and $\mathbf{S}$ do not change with different transmitted data. Then, calculating $\mathbf{I}+\lambda\mathbf{T}_\mathbf{w}^H\mathbf{S}^H\mathbf{S}\mathbf{T}_\mathbf{w}$ needs $2N_w^2$ real multiplications; calculating its inversion needs another $2N_w^3$ real multiplications using, for example, Cholesky Decomposition [25]. Calculating $(\check{\mathbf{w}}-\lambda\mathbf{T}_\mathbf{w}^H\mathbf{S}^H\mathbf{S}\mathbf{d})$ needs $2N_w$ real multiplications, given that $\mathbf{T}_\mathbf{w}^H\mathbf{S}^H\mathbf{S}\mathbf{d}$ is ready at the start of the algorithm. Calculating $(\mathbf{I}+\lambda\mathbf{T}_\mathbf{w}^H\mathbf{S}^H\mathbf{S}\mathbf{T}_\mathbf{w})^{-1}(\check{\mathbf{w}}-\lambda\mathbf{T}_\mathbf{w}^H\mathbf{S}^H\mathbf{S}\mathbf{d})$ needs another $4N_w^2$ real multiplications to multiply an $N_w\times N_w$ complex matrix with an $N_w\times 1$ complex vector. Suppose that it takes K iterations for Algorithm 3 to converge. It requires $K(2N_w^3+6N_w^2+2N_w)$ real multiplications for the projection onto Set $\mathcal{A}$. We assume that $(\mathbf{I}+\lambda\mathbf{T}_\mathbf{w}^H\mathbf{S}^H\mathbf{S}\mathbf{T}_\mathbf{w})^{-1}$ is pre-calculated and stored with a set of λ's. The number of real multiplications is calculated as $K(4N_w^2+2N_w)$. The computational complexity of the projection onto Set $\mathcal{A}$ is $O(N_w^2)$.

In Algorithm 1 and Algorithm 2, the projection onto Set $\mathcal{B}$ requires standard convex optimization tools. It usually has high computational complexity and is hard to analyze. Similar to the computational complexity analysis in [15], [26], the projection onto the set control by the PAPR requirement can be reformulated as a second-order cone program (SOCP). The problem can be solved by the standard interior-point method, and the computational complexity is $O(N^3)$ in each iteration. Besides, one IDFT operation is needed during each iteration, which has the complexity of $O(JN\log JN)$. Therefore, the computational complexity of the projection onto Set $\mathcal{B}$ is $O(N^3+JN\log JN)$. The computational complexity of the projection onto Set $\mathcal{A}$ is much smaller than that of the projection onto Set $\mathcal{B}$. In order to reduce the algorithm complexity, a simple method of time-domain clipping can be applied to limit the PAPR, but the PAPR performance will drop.

4. Simulation Results

An NC-OFDM system is simulated with an OFDM symbol of 64 subcarriers. There are three non-contiguous frequency blocks that occupy the subcarriers indexed 0 to 15, 24 to 39, and 48 to 63. The cognitive-radio secondary users transmit QPSK signals over these subcarriers. The other OFDM subcarriers are used for the incumbent primary users of the spectrum. In particular, the frequency bands over subcarriers indexed 16 to 23 and 40 to 47 are used by the primary users. The interference to these bands needs to be reduced. To measure the OBP in these two frequency bands, a total of 512 frequency samples $\{g_m\}$ are taken such that each band has 256 evenly spaced frequency samples. In order to combat the OBP and the PAPR, the subcarriers of the secondary users indexed 0, 5, 10, 15, 24, 29, 34, 39, 48, 53, 58, 63 and the subcarriers of the primary users are selected to carry adjusting weights. In this simulation setting, the overhead is 25% of the NC-OFDM subcarriers. On the one hand, this is the cost of the secondary users if they use the spectrum. On the other hand, the 64-subcarrier OFDM symbol is simulated for clarity. In a practical system, more subcarriers can be used to lower the overhead percentage. The length of the cyclic prefix $N_{cp}=16$. When calculating the PAPR, we set oversampling factor $J=4$. The interpolation filter $g_I(t)$ is the ideal low-pass filter, and no other out-of-band power suppression methods are applied. The adjusting weights are initialized to zero.

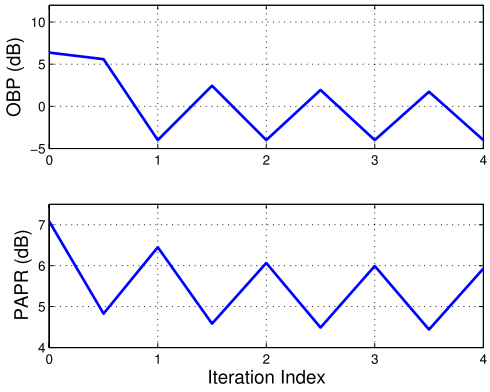

Fig. 3 POCS process of Algorithm 1 when there is no intersection between Set $\mathcal{A}$ and Set $\mathcal{B}$.

The joint reduction of the OBP and the PAPR is achieved using the method of POCS. In Algorithm 1, the projection onto Set $\mathcal{A}$ regulated by the OBP requirement is calculated by Algorithm 3. The projection onto Set $\mathcal{B}$ regulated by the PAPR requirement is calculated with convex optimization tools. Figure 3 shows the OBP and the PAPR over the iterations of the algorithm when $P_{\text{OBP}}=-4$ dB and $\Gamma_{\text{PAPR}}=5$ dB. The limits are set so that $\mathcal{A}$ and $\mathcal{B}$ have no intersection. The PAPR and the OBP are calculated after Step 2 and 3 of Algorithm 1. Because $\mathcal{A}$ and $\mathcal{B}$ have no intersection, the OBP and the PAPR values oscillate at each projection. If Algorithm 1 terminates at a vector point on $\mathcal{A}$, the solution has an OBP within -4 dB.

The performances of the proposed algorithms are compared with the performance of the constellation extension (CE) method for joint PAPR reduction and sidelobe suppression in NC-OFDM systems. In Fig. 4 and Fig. 5, $\text{CCDF}(\text{PAPR}_0)=\Pr\{\text{PAPR}>\text{PAPR}_0\}$, and $\text{CCDF}(\text{OBP}_0)=\Pr\{\text{OBP}>\text{OBP}_0\}$. It should be noted that the CE method used in our simulation minimizes the OBP with the constraint on the PAPR instead of minimizing the PAPR as in [15]. The parameter in the CE method is set such that $\mu=0.333$, which means that the transmit power can be increased to 1.333 times of the original power, which can be regarded as reserving 25% transmit power by the CE method. In the simulations, we adjust the PAPR reduction performance of the CE method such that it is comparable with the proposed algorithms. In order to avoid empty set constrained by the PAPR in the proposed algorithms, the PAPR limit cannot be set too small, and $\Gamma_{\text{PAPR}}=8$ dB in the simulations. The OBP limits are set as $P_{\text{OBP}}=0$ dB and $P_{\text{OBP}}=-4$ dB for Algorithm 1 and Algorithm 2, respectively. Algorithm 1 cannot achieve the same PAPR reduction

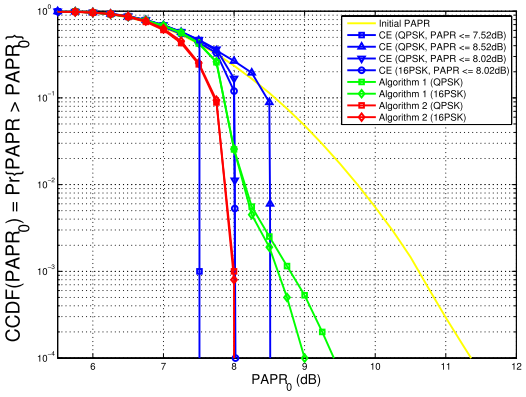

Fig. 4 Complementary cumulative distribution of PAPR.

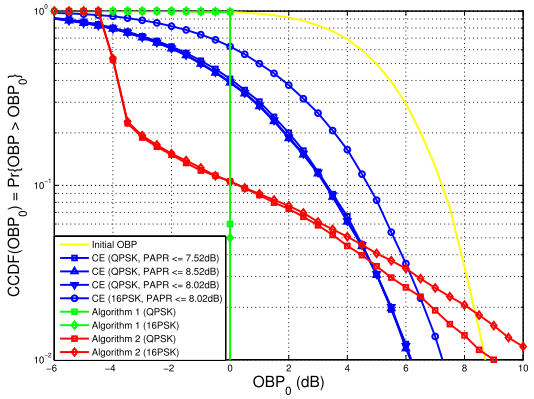

Fig. 5 Complementary cumulative distribution of OBP.

performance as the CE method and Algorithm 2, because the OBP reduction has higher priority for Algorithm 1. When CCDF = 0.001 and QPSK is employed, the PAPR of Algorithm 1 and Algorithm 2 is 8.8 dB and 8 dB, respectively. For the CE method, the PAPR reduction performance is better because all the tones can be used to control the PAPR, while for Algorithm 1 and Algorithm 2 only a part of the subcarriers accommodate adjusting weights. But with similar PAPR reduction performance, the proposed algorithms have better OBP reduction performance than the CE method. It is because, for the CE method, the constellation points can only be extended in specific directions in order to allow the receiver to decode the data correctly. It should be noted that in Fig. 4 some parts of the PAPR performance are vertical lines. This is because that for CE method and Algorithm 2, the PAPR is limited within the constraints. In addition, we simulate the algorithms with different constellation sizes. It can be shown in Fig. 4 and Fig. 5, the proposed algorithms have similar PAPR and OBP reduction performance with different constellation sizes. But, since the constellation points can only be extended in smaller regions because of the larger constellation size, the OBP reduction performance of the CE method is degraded. This is consistent with the findings in [27] that the increase in constellation size results in low performance gain in the CE method.

Figure 6 and Fig. 7 show the impact of the target OBP

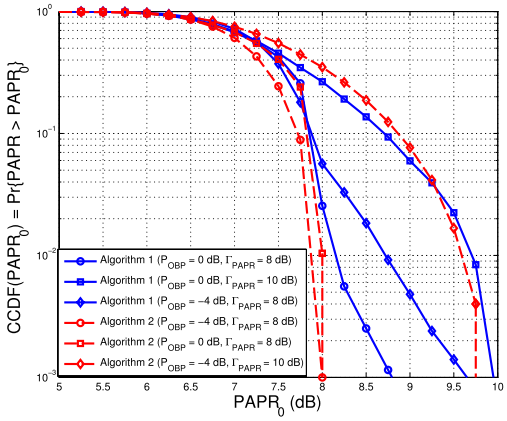

Fig. 6 Complementary cumulative distribution of PAPR.

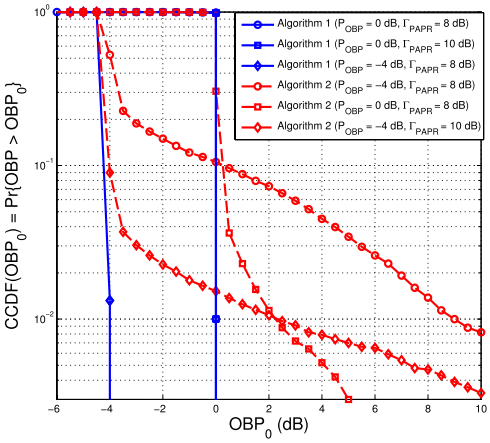

Fig. 7 Complementary cumulative distribution of OBP.

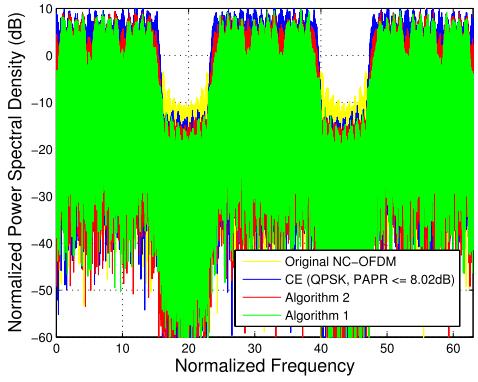

Fig. 8 Power spectrum density of the NC-OFDM signals with the proposed algorithms and the CE method.

and PAPR. For Algorithm 1, the OBP performance is determined by P_{OBP}. With the same Γ_{PAPR}, looser target OBP limit causes better PAPR performance. For Algorithm 2, the PAPR performance is determined by Γ_{PAPR}. With the same P_{OBP}, looser target PAPR causes better OBP performance.

Figure 8 shows the normalized power spectrum density (PSD) of the NC-OFDM signals with the proposed algorithms and the CE method. When calculating the PSD, 10^4

independent NC-OFDM symbols modulated by QPSK are randomly generated. The Welch method with Blackman window is used to calculate the PSD of the transmitted NC-OFDM signals. It is shown that Algorithm 1 can improve the OBP suppression in the two dedicated frequency bands by about 7 dB. The better OBP performance of Algorithm 1 is at the cost of the PAPR performance.

5. Conclusion

NC-OFDM can be used for cognitive radio systems. But the drawbacks of the high OBP leakage and the high PAPR need to be overcome. In this paper, the methods that select several NC-OFDM subcarriers to accommodate weights are proposed. These weights adjust the OBP and the PAPR. The algorithms of joint reduction of the OBP and the PAPR are based on the alternating projections onto convex sets. The frequency-domain NC-OFDM symbol is regarded as the projected vector and the convex sets are defined by the OBP and PAPR requirements. The properties of the POCS guarantee the convergence of the proposed algorithms. The solution signal vector satisfies either the OBP or the PAPR requirement and is closest to the set constrained by the other requirement. The performances of the proposed algorithms are compared with those of the method based on constellation extension.

References

[1] H. Bogucka, A.M. Wyglinski, S. Pagadarai, and A. Kliks, "Spectrally agile multicarrier waveforms for opportunistic wireless access," IEEE Commun. Mag., vol.49, no.6, pp.108–115, June 2011.
[2] D. Qu, J. Ding, T. Jiang, and X. Sun, "Detection of non-contiguous OFDM symbols for cognitive radio systems without out-of-band spectrum synchronization," IEEE Trans. Wireless Commun., vol.10, no.2, pp.693–701, Feb. 2011.
[3] X. Li, V.D. Chakravarthy, B. Wang, and Z. Wu, "Spreading code design of adaptive non-contiguous SOFDM for dynamic spectrum access," IEEE J. Sel. Topics Signal Process., vol.5, no.1, pp.190–196, Feb. 2011.
[4] I. Cosovic and T. Mazzoni, "Suppression of sidelobes in OFDM systems by multiple-choice sequences," Eur. Trans. Telecommun., vol.17, no.6, pp.623–630, Nov. 2006.
[5] Z. Yuan and A.M. Wyglinski, "On sidelobe suppression for multicarrier-based transmission in dynamic spectrum access networks," IEEE Trans. Veh. Technol., vol.59, no.4, pp.1998–2006, May 2010.
[6] S. Pagadarai, R. Rajbanshi, A.M. Wyglinski, and G.J. Minden, "Sidelobe suppression for OFDM-based cognitive radios using constellation expansion," Proc. IEEE Wireless Commun. Netw. Conf. (WCNC), pp.888–893, April 2008.
[7] D. Li, X. Dai, and H. Zhang, "Sidelobe suppression in NC-OFDM systems using constellation adjustment," IEEE Commun. Lett., vol.13, no.5, pp.327–329, May 2009.
[8] J.A. Zhang, X. Huang, A. Cantoni, and Y.J. Guo, "Sidelobe suppression with orthogonal projection for multicarrier systems," IEEE Trans. Commun., vol.60, no.2, pp.589–599, Feb. 2012.
[9] H.A. Mahmoud and H. Arslan, "Sidelobe suppression in OFDM-based spectrum sharing systems using adoptive symbol transition," IEEE Commun. Lett., vol.12, no.2, pp.133–135, Feb. 2008.
[10] J. van de Beek, "Orthogonal multiplexing in a subspace of frequency well-localized signals," IEEE Commun. Lett., vol.14, no.10, pp.882–884, Oct. 2010.
[11] B.S. Krongold and D.L. Jones, "An active-set approach for OFDM PAR reduction via tone reservation," IEEE Trans. Signal Process., vol.52, no.2, pp.495–509, Feb. 2004.
[12] X. Li and L.J. Cimini, "Effect of clipping and filtering on the performance of OFDM," IEEE Commun. Lett., vol.2, no.5, pp.131–133, May 1998.
[13] M. Senst, M. Jordan, M. Dorpinghaus, M. Farber, G. Ascheid, and H. Meyr, "Joint reduction of peak-to-average power ratio and out-of-band power in OFDM systems," Proc. IEEE Global Commun. Conf. (GLOBECOM), pp.3812–3816, Nov. 2007.
[14] A. Ghassemi, L. Lampe, A. Attar, and T.A. Gulliver, "Joint sidelobe and peak power reduction in OFDM-based cognitive radio," Proc. IEEE Veh. Technol. Conf. (VTC), pp.1–5, Sept. 2010.
[15] C. Ni, T. Jiang, and W. Peng, "Joint PAPR reduction and sidelobe suppression using signal cancelation in NC-OFDM-based cognitive radio systems," IEEE Trans. Veh. Technol., vol.64, no.3, pp.964–972, March 2015.
[16] Y. Liu, L. Dong, and R.J. Marks, "Joint reduction of out-of-band power and peak-to-average power ratio for non-contiguous OFDM systems," Proc. IEEE Global Commun. Conf. (GLOBECOM), pp.3493–3498, Dec. 2013.
[17] F.J. Harris, "On the use of windows for harmonic analysis with the discrete Fourier transform," Proc. IEEE, vol.66, no.1, pp.51–83, Jan. 1978.
[18] T. van Waterschoot, V. Le Nir, J. Duplicy, and M. Moonen, "Analytical expressions for the power spectral density of CP-OFDM and ZP-OFDM signals," IEEE Signal Process. Lett., vol.17, no.4, pp.371–374, April 2010.
[19] G. Cuypers, K. Vanbleu, G. Ysebaert, and M. Moonen, "Intra-symbol windowing for egress reduction in DMT transmitters," EURASIP J. Adv. Sigal Process., vol.2006, Artical ID 70387, 2006.
[20] D.C. Youla and H. Webb, "Image restoration by the method of convex projections: Part 1 – theory," IEEE Trans. Med. Imag., vol.MI-1, no.2, pp.81–94, Oct. 1982.
[21] M. Goldburg and R.J. Marks II, "Signal synthesis in the presence of an inconsistent set of constraints," IEEE Trans. Circuits Syst., vol.32, no.7, pp.647–663, July 1985.
[22] R.J. Marks, Handbook of Fourier Analysis & Its Applications, Oxford University Press, 2009.
[23] D.C. Youla and V. Velasco, "Extensions of a result on the synthesis of signals in the presence of inconsistent constraints," IEEE Trans. Circuits Syst., vol.33, no.4, pp.465–468, April 1986.
[24] S. Boyd and L. Vandenberghe, Convex Optimization, Cambridge University Press, 2004.
[25] A. Krishnamoorthy and D. Menon, "Matrix inversion using Cholesky decomposition," Signal Processing: Algorithms, Architectures, Arrangements, and Applications (SPA), 2013, pp.70–72, Sept. 2013.
[26] Y. Wang and Z. Luo, "Optimized iterative clipping and filtering for papr reduction of OFDM signals," IEEE Trans. Commun., vol.59, no.1, pp.33–37, Jan. 2011.
[27] B. Krongold and D. Jones, "Par reduction in OFDM via active constellation extension," IEEE Trans. Broadcast., vol.49, no.3, pp.258–268, April 2003.

Yanqing Liu received the B.S. degree in applied electronics and the M.S. degrees in signal and information processing from Northwestern Polytechnical University, China, in 2000 and 2003, and the Ph.D. degree in electrical and computer engineering from Baylor University, U.S.A, in 2015. From 2003 to 2011, he worked as senior hardware engineer, senior software engineer and manger of driver software department respectively, in Datang Mobile Communications Equipment Company Limited, where he participated in the design of TD-SCDMA and TD-LTE system. Presently, he is with the Department of Communication Engineering, Jiangxi University of Finance and Economics. His research interests include cognitive radio network, communication systems, wireless networks, digital signal processing, and cyber-physical systems.

Liang Dong received the B.S. degree in applied physics with minor in computer engineering from Shanghai Jiao Tong University, China, in 1996, and the M.S. and Ph.D. degrees in electrical and computer engineering from The University of Texas at Austin in 1998 and 2002, respectively. From 2002 to 2004, he was a Research Associate with the Department of Electrical Engineering, University of Notre Dame. From 2004 to 2011, he was an Assistant Professor then promoted to a tenured Associate Professor of the Department of Electrical and Computer Engineering at Western Michigan University. He joined the faculty of Baylor University in August 2011 as an Associate Professor of Electrical and Computer Engineering. His research interests include communication systems, wireless networks, digital signal processing, cyber-physical systems, and microelectronics for communications.